ENHANCED THERMAL PERFORMANCE OF A WATER-COOLED COLD PLATE WITH POROUS INSERTS FABRICATED BY SELECTIVE LASER MELTING

Ho J.Y. and Leong K.C. *
*Author for correspondence
Singapore Centre for 3D Printing
School of Mechanical and Aerospace Engineering
Nanyang Technological University
50 *Nanyang Avenue*
Singapore 639798
Republic of Singapore
E-mail: mkcleong@ntu.edu.sg

ABSTRACT

The paper presents an experimental investigation of the thermal and hydraulic performance of a new class of porous metallic foams with ordered arrangements of the Rhombi-Octet unit cell design for use in a water-cooled cold plate. Selective laser melting (SLM) was employed to fabricate the porous metallic foams of two different unit cell sizes. A closed-loop chilled water test facility was set up to perform the experimental investigation and the results of the SLM fabricated porous metallic foams were compared with those of a commercially available metallic foam of random tetrakaidecahedron-like unit cell structures. The permeability (K) and inertia coefficient (C_E) of the various metallic foams were characterized using the Forchheimer-extended Darcy equation and it was determined that K can be enhanced by 3.3 times with an increase in unit cell size of the Rhombi-Octet design from 5 mm to 10 mm. In addition, the Rhombi-Octet metallic foam insert also exhibits up to 91% enhancement in the heat transfer coefficient (h_{ave}) as compared to the empty channel cold plate and up to 47% as compared to the commercial metallic foam insert.

INTRODUCTION

Liquid-cooled cold plates are commonly employed in the thermal management of electronic components. They consist of a heat spreading surface on which the heat source is mounted and internal flow channels which dissipate heat by single-phase forced convection. Water is the preferred cooling medium as it is readily available and has better thermophysical properties as compared to many other coolants.

Due to the increasing need for higher heat flux dissipation, thermal enhancement techniques for cold plates have been widely investigated. One passive single-phase heat transfer enhancement technique is the introduction of surface features such as twisted tapes [1], internal finned structures [2] and microchannels [3] where improvements in heat transfer performances were reported. In addition to these surface features, the use of metallic porous foams in augmenting the thermal performance of heat transfer devices has also received significant attention in recent years [4, 5]. The main advantages of metallic porous foams are their high effective thermal conductivity and high packing density which increase the overall heat transfer surface. In addition, the porous network also induced tortuous fluid paths which intensify and perpetuate fluid mixing.

NOMENCLATURE

h_{ave}	[W/m^2·K]	Length-averaged heat transfer coefficient
C_E	-	Inertia coefficient
K	[m^2]	Permeability
k_d	[W/m·K]	Thermal dispersion conductivity
L	[mm]	Length of flow channel
$\dot{m}$	[kg/s]	Mass flow rate
ΔP	[Pa]	Pressure drop
$\dot{q}$	[W/m^2]	Heat flux
T	[ºC]	Temperature
U	[m/s]	Average flow velocity
Greek Letters		
μ	[kg/m·s]	Dynamic viscosity
ρ	[kg/m^3]	Density
Subscripts		
f		Fluid
in		Inlet
out		Outlet

Due to these advantages, the thermal performances of metallic porous foams have been extensively studied. For instance, Leong and Jin [4] assessed the performance of metallic foams of approximately 90% porosity and different pores per inch (PPI) under steady and oscillating flow conditions and determined that they were more superior in thermal performance than conventional finned heat sinks. Boomsma and Poulikakos [6] showed that heat exchangers with compressed porous foams (between 60 - 90% porosity) could reduce thermal resistance by almost half as compared to commercial heat exchangers. In addition, significant reductions in thermal resistance were observed at constant pumping power. More recently, Chen and Wang [7] explored the performance of liquid-cooled heat sinks that were partially filled with metallic foams. In their studies, metallic foams of constant and varying PPIs were periodically arranged in the flow channel at 10 mm spacing. Their results showed that at

constant pumping power, the heat sinks with metallic foams reduced their thermal resistance by 44 - 62% as compared to an empty channel

However, investigations in single-phase heat transfer of metallic foams were largely limited to random arrangements of tetrakaidecahedron-like unit cell structures [6, 8, 9]. In this paper, a new class of metallic foams with ordered arrangements of Rhombi-Octet unit cell structure for enhancing the thermal performance of a water-cooled cold plate was investigated. Selective laser melting (SLM), an additive manufacturing technique, was employed to fabricate the metallic foams of different unit cell sizes and their thermal and hydraulic performances were experimentally investigated. The performance of the SLM fabricated metallic foams were also compared with a commercial metallic foam with a Tetrakaidecahedron-like structure and an empty flow channel cold plate. Our results show that the better performing Rhombi-Octet metallic foam insert enhanced the heat transfer coefficient (h_{ave}) by up to 91% as compared to the empty channel cold plate and by up to 47% compared to the commercial metallic foam insert.

FABRICATION AND CHARACTERIZATION OF METALLIC FOAMS

The metallic foams employed in the present investigation were fabricated using the SLM 250 HL (SLM Solutions GmbH) facility in the Singapore Centre for 3D Printing of Nanyang Technological University, Singapore. Aluminum alloy (AlSi10Mg) powder of 20 µm to 63 µm size distribution was used. A Gaussian distributed Yb:YAG laser with a maximum power of 400 W and a laser beam spot size of 80 µm was utilized to melt and fuse the powder layer-by-layer based on the input of a Computer Aided Design (CAD) model. A laser power of 350 W, scanning speed of 1150 mm/s and hatching spacing of 0.17 mm were used. The unit cell of the Rhombi-Octet structure is shown in Fig. 1 (a) and the fabricated metallic foam of 5 mm unit cell size is depicted in Fig. 1 (b). In total, two Rhombi-Octet metallic foams (*M*1 and *M*2) with overall dimensions of 90 mm × 40 mm × 10 mm were produced. In addition, a commercial aluminum foam (*P*) manufactured by Duocel®, as shown in Fig. 1 (c), of the same overall dimensions was selected for comparison. A comparison of the Rhombi-Octet structure and the Tetrakaidecahedron-like structure taken from the OLYMPUS SZX7 Stereo Microscope is shown in Fig. 2 and the geometric parameters of the metallic foams tested are summarized in Table 1. It can be seen that due to the higher packing density of the Rhombi-Octet unit cell structure as compared to the commercial metallic foam, a lower porosity and similar surface area-to-volume ratio can be achieved with larger ligament width and length. In the present investigation, a cold plate with a rectangular flow channel of dimensions similar to that of the metallic foams was prepared. Prior to the experiments, the metallic foams were forced-fitted into the flow channel and nine K-type thermocouples (T_1 to T_9) were inserted at locations which are 1.5 mm below the heated surface of the cold plate as shown in Fig. 3. The thermocouple readings were then used to compute the length-averaged wall temperature (T_w) as shown in Eq. (1).

$$T_w = \frac{1}{\Delta L}\int_{L_1}^{L_2} T_x\, dx \approx \frac{1}{2N}\sum_{k=1}^{N}(T_{k+1} + T_k) \quad (1)$$

where $N = 8$.

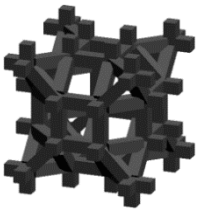

(a)

(b)

(c)

Figure 1. (a) Rhombi-Octet unit cell, (b) image of Rhombi-Octet metallic foam (*M*1), and (c) image of commercial aluminum foam (*P*).

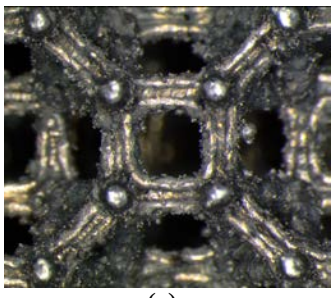

(a)

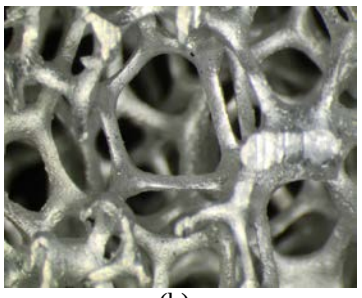

(b)

Figure 2. Microscopic images of (a) Rhombi-Octet structure (*M*1) and (b) Tetrakaidecahedron-like structure (*P*).

Table 1. Parameters of metallic foams investigated

No.	Unit cell size (mm)	Ligament width (mm)	Ligament length (mm)	Ligament width-to-length ratio	Porosity	Surface area-to-volume ratio (m^2/m^3)
*M*1	5	0.40	1.8	0.22	0.85	1488
*M*2	10	0.80	3.6	0.22	0.85	744
P	-	0.25	0.9	0.28	0.9	1700

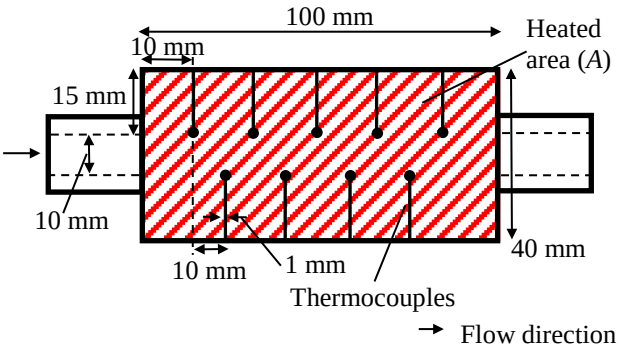

Figure 3. Schematic of cold thermocouple locations

EXPERIMENTAL SETUP AND PROCEDURES

The experimental investigations of the cold plates were conducted with a closed-loop chilled water circuit as shown in Fig. 4. A variable speed gear pump was employed to provide the required water flow velocity (*U*) through the cold plates. A fully-filled water tank (250 mm × 250 mm × 250 mm) with an in-built heat exchanger coil which is connected to a chiller allows the inlet water to flow into the cold plate to maintain the required temperature. Two resistance temperature detectors (RTDs), located at 200 mm upstream and downstream of the cold plate, were used to measure the cold plate water inlet (T_{in}) and outlet (T_{out}) temperatures. A turbine flowmeter were installed after the pump to obtain the average water flow velocity (*U*) and a differential pressure transducer was also installed to determine the pressure drop across the cold plate (ΔP). The connecting pipes of internal diameter 10 mm were insulated with elastomeric foam to minimize heat loss to the surroundings. All RTDs, thermocouples, flow meter and pressure transducers were connected to a data acquisition system (Yokogawa MX100) where the readings were recorded.

The heater section and cold plate are shown in Fig. 5. It consists of a copper block (100 mm × 40 mm × 12 mm) heat spreader which was mounted onto the top side of the cold plate. Four 6.35 mm-diameter cartridge heaters (each of 250 W rated power) were used as the heat source and these were inserted into the copper block. Teflon of external dimensions 120 mm × 70 mm × 70 mm was used as the insulation material to enclose the copper block on all the other sides to minimize heat loss. The cartridge heaters were connected to a variable transformer which allowed the heat output from the cartridge heaters to be varied. To reduce the thermal contact resistance, a thin layer of thermal grease was applied at the cold plate and the copper block interfaces.

Using T_{out} and T_{in} recorded from the RTDs and the fluid mass flow rate ($\dot{m}$) computed from the fluid flow meter, the total rate of heat dissipated from the cold plate ($\dot{q}$) is determined using Eq. (2), where *A* denotes the area of the heated surface. Finally, by energy conservation, the length-averaged heat transfer coefficient (h_{ave}) of the cold plate is determined from Eq. (3) where T_w is determined from Eq. (1). The maximum uncertainties of *U*, h_{ave} and ΔP were determined to be ± 3%, ± 5.9% and ± 10.9%, respectively.

$$\dot{q} = \frac{\dot{m} c_{p,f} (T_{out} - T_{in})}{A} \tag{2}$$

$$h_{ave} = \frac{\dot{m} c_{p,f} (T_{out} - T_{in})}{A \left[T_w - \frac{T_{out} + T_{in}}{2} \right]} \tag{3}$$

RESULTS AND DISCUSSION

The pressure drop, ΔP, across the cold plate filled with various metallic foams for different velocities, *U*, are shown in Fig. 6. It can be observed that the metallic foam with smaller unit cell size (*M*1) resulted in significantly larger ΔP values whereas relatively similar ΔP values were recorded for *P* and *M*2. In addition, ΔP also vary as quadratic functions of *U*, suggesting that the flow lies within the non-Darcy regime. Hence, using the Forchheimer-extended Darcy equation as shown in Eq. (4) [10], the permeability (*K*) and drag coefficient (C_E) of the metallic foams employed in the present flow channel were determined and summarized in Table 2. It can be seen that the C_E values of the cold plates are relatively similar although significant differences in their *K* values can be observed. Both *M*1 and *M*2 have the same unit cell design and porosity. However, the increase in unit cell size from 5 mm (for *M*1) to 10 mm (for *M*2) has resulted in the increase in the ligament diameter and pore size of the porous structure which enhanced its permeability by 3.3 times.

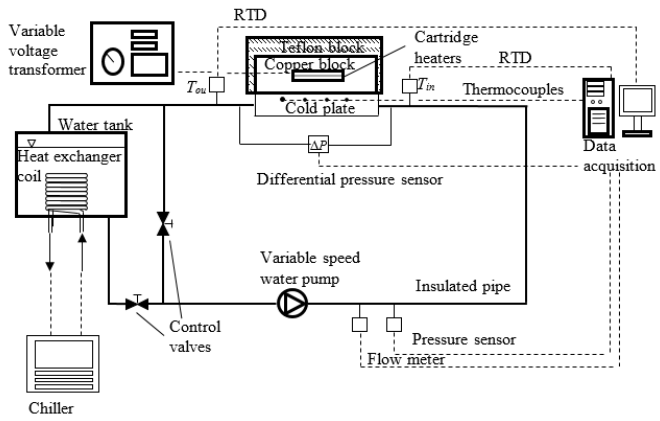

Figure 4. Schematic of experimental setup.

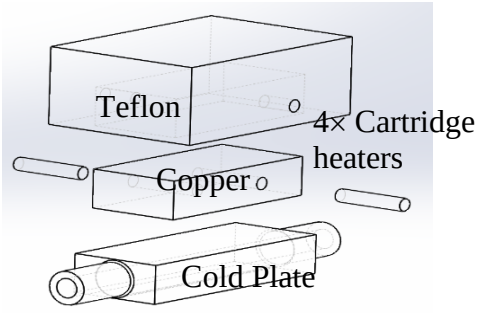

Figure 5. Schematic of heater section and cold plate.

$$\frac{\Delta P}{L} = \frac{\mu_f}{K} U + \frac{\rho_f C_E}{\sqrt{K}} U^2 \qquad (4)$$

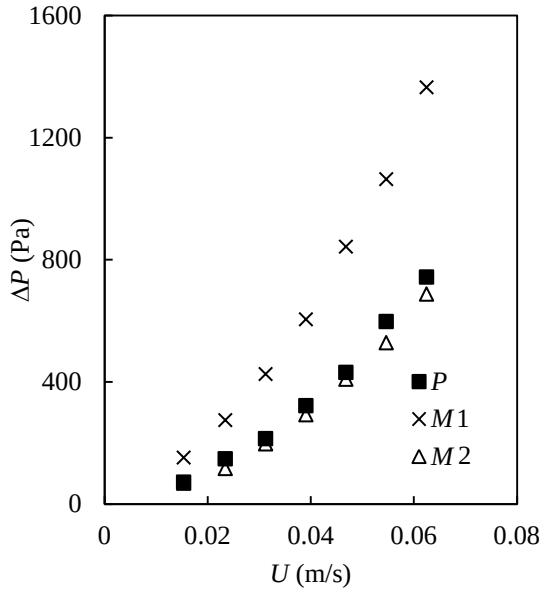

Figure 6. Comparison of cold plate pressure drops at different fluid velocities.

Table 2 K and C_E of various cold plates.

	K (10^{-8} m^2)	C_E
$M1$	1.61	0.36
$M2$	5.25	0.38
P	4.15	0.35

The local heat transfer coefficients (h_x) computed based on the localized wall temperature measurements (T_1 to T_9) at U = 0.15 m/s, 0.39 m/s and 0.63 m/s are depicted in Fig. 7, where x/L denotes the dimensionless axial distance from the water inlet (x/L = 0) to outlet (x/L = 1). Due to the contraction and expansion of the fluid at the inlet and outlet of the cold plate, noticeably higher h_x values were recorded at x/L = 0.1 and x/L = 0.9 for all cold plates. The h_x values of the cold plates gradually decrease with increase of x/L where the lowest h_x values were recorded at approximately x/L = 0.5. As the thermally developed regime was achieved, the h_x values remained relatively constant between x/L = 0.5 and 0.7. Comparing Fig. 7 (a), (b) and (c), it can be observed that the difference between the h_x curves of the Rhombi-Octet foams ($M1$ and $M2$) and that of the commercial foam (P) also increases with increasing water velocity (U) with $M1$ and $M2$ exhibiting better thermal performances than P.

The average heat transfer coefficients (h_{ave}) of the empty channel cold plate and the various metallic foams are shown in Fig. 8. It can be seen that the metallic foams significantly increased the h_{ave} values of the cold plates, with $M2$ exhibiting the highest enhancements in h_{ave} of up to 91% as compared to the empty channel cold plate at U = 0.15 m/s. The highest h_{ave} values of 4113 W/m^2·K was also achieved with the $M2$ porous foam. In addition, the results also show that the thermal performance of the Rhombi-Octet structures consistently surpasses that of the commercial foam and the magnitude of enhancement in h_{ave} increases with increasing U values. The highest enhancement in h_{ave} of 47% as compared to the commercial foam was achieved with $M2$ at U = 0.63 m/s. The enhancement can be attributed to the higher packing density of the new Rhombi-Octet design which intensified the tortuous fluid paths and improved fluid mixing.

Both $M1$ and $M2$ consist of the same unit cell design. However, in comparison to $M1$, $M2$ demonstrated noticeably better heat transfer performance and lower pressure drop over the whole range of fluid velocities tested. Several studies have shown that the enhancements in the heat transfer performance of metallic foams can be attributed to the improved dispersion conductivity (k_d) where k_d was shown to be directly proportional to the square root of permeability ($\sqrt{K}$) of the porous medium [11]. It can be seen from Table 2 that significantly larger K values were obtained for $M2$ as compared to $M1$, suggesting that the higher heat transfer performance of $M2$ was achieved due to better thermal dispersion.

In all, the present investigation demonstrates that higher thermal performance can be achieved with ordered arrangements of Rhombi-Octet unit cell design as compared to an empty channel cold plate and random arrangements of

Tetrakaidecahedron-like unit cell structures of the commercial porous foam. Likely due to the ordered unit cell arrangement, a ΔP value similar to that of the commercial foam was also achieved with $M2$ even though the porosity of $M2$ is relatively lower.

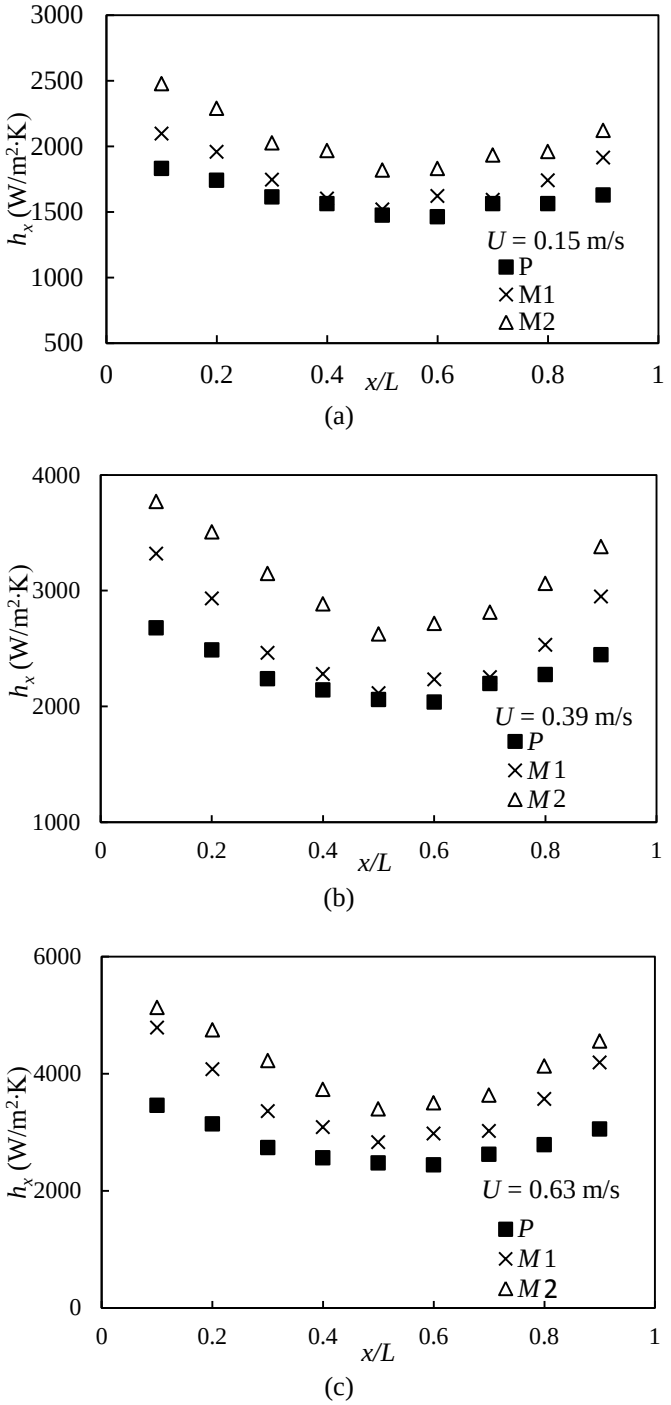

Figure 7. Comparison of cold plate local transfer coefficients at different fluid velocities (a) U = 0.15 m/s, (b) U = 0.39 m/s and (c) U = 0.63 m/s.

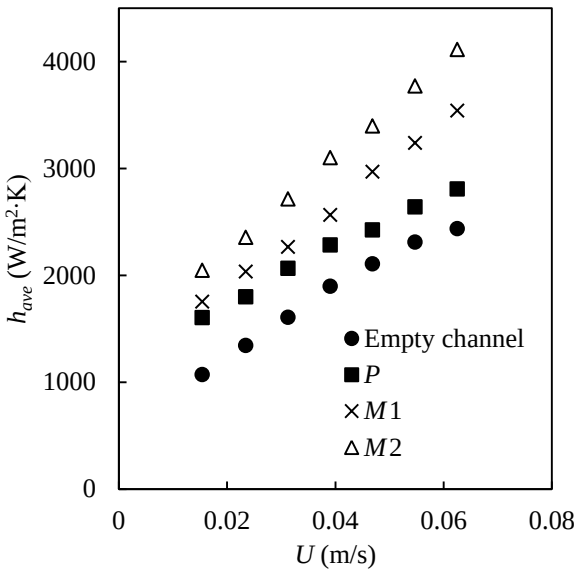

Figure 8. Comparison of cold plate heat transfer coefficients at different fluid velocities.

CONCLUSION

The thermal and hydraulic performances of 3D printed metallic foams with the Rhombi-Octet structure in a water-cooled cold plate were investigated experimentally. The results show that the h_{ave} values of these metallic foams are higher than that of a commercially available metallic foam. In addition, the best performing Rhombi-Octet metallic foam ($M2$) exhibits up to 91% enhancement in h_{ave} as compared to an empty channel cold plate and significantly lower pressure drop ΔP as compared to other metallic foams.

ACKNOWLEDGMENT

Funding for the SLM facility by the National Research Foundation, Singapore, is gratefully acknowledged.

REFERENCES

[1] Manglik, R.M., Bergles, A.E., Heat transfer and pressure drop correlations for twisted-tape inserts in isothermal tubes: Part I- Laminar Flows, *Journal of Heat Transfer,* Vol. 115, pp. 881-889 (1993).

[2] Lee, Y.J., Lee, P.S., Chou, S.K., Enhanced thermal transport in microchannel using oblique fins, *Journal of Heat Transfer,* Vol. 134, pp. 101901-1 – 101901-10 (2012).

[3] Vanapalli, S., ter Brake, H.J.M., Jansen, H.V., Burger, J.F., Holland, H.J., Veenstra, T.T, Elwenspoek, M.C., Pressure drop of laminar gas flows in a microchannel containing various pillar matrices, *Journal of Micromechanics and Microengineering,* Vol. 17, pp. 1381-1386 (2007).

[4] Leong, K.C., Jin, L.W., Effect of oscillatory frequency on heat transfer in metal foam heat sinks of various

pore densities, *International Journal of Heat and Mass Transfer*, Vol. 49, pp. 671-681 (2006).

[5] Dukhan, N., Bağci, Ö., Özdemir, M., Thermal development in open-cell metal foam: An experiment with constant wall heat flux, *International Journal of Heat and Mass Transfer*, Vol. 85, pp. 852-859 (2015).

[6] Boomsma, K., Poulikakos, D., On the effective thermal conductivity of a three-dimensionally structured fluid-saturated metal foam, *International Journal of Heat and Mass Transfer*, Vol. 44, pp. 827-836 (2000).

[7] Chen, K.-C., Wang, C.-C., Performance improvement of high power liquid-cooled heat sink via non-uniform metal foam arrangement, *Applied Thermal Engineering*, Vol. 87, pp. 41-46 (2015).

[8] Dai, Z., Nawaz, K., Park, Y.G., Bock, J., Jacobi, A.M., Correcting and extending the Boomsma-Poulikakos effective thermal conductivity model for three-dimensional, fluid saturated metal foams, *International Communications in Heat and Mass Transfer*, Vol. 37, pp. 575-580 (2010).

[9] Yang, H., Zhao, M., Gu, Z.L., Jin, L.W., Chia, J.C., A further discussion on the effective thermal conductivity of metal foam: An improved model, *International Journal of Heat and Mass Transfer*, Vol. 86, pp. 207-211 (2015).

[10] Dupuit, J., *Etudes Théoriques et Pratiques sur le Mouvement des Eaux dans les Canaux Découverts et à Travers les Terrains Perméables*, 2*ème édition*, Dunod, Paris, 1863 (in French).

[11] Hunt, M.L., Tien, C.L., Effects of thermal dispersion on forced convection in fibrous media, *International Journal of Heat and Mass Transfer*, Vol. 31, pp. 301-309 (1998).